International Journal of Fluid Power 4 (2003) No. 3 pp. 47-56

IMPROVING GAS DYNAMIC MODELS FOR PNEUMATIC SYSTEMS

Salvador de las Heras

Department of Fluid Mechanics. Universidad Politécnica de Cataluña. Campus of Terrassa. C/Colom 7-11 E08222 Terrassa - Spain
delasheras@mf.upc.es

Abstract

The present paper deals with the improvement to modelling of pneumatic systems. The thermal air process inside the pneumatic chambers is modelled without using the polytrophic exponent to relate the pressure-density relationship. The model takes into account the real gases behaviour and the thermal constant time for estimating heat transfer. The polytrophic exponent is used only for adjusting the data and to improve the understanding of the system. The validity of this method is demonstrated by experiments.

Keywords: pneumatics, gas compression process, compressible fluid-flow, polytrophic index, simulation

1 Introduction

The pneumatic technology is widely used throughout manufacturing industry to provide linear motion, medium force applications. Low cost pneumatic actuators are cheaper, fast enough and they avoid pollution in the event of external fluid leakage. This technology can present a real advantage for positioning systems but, until now, it has been essentially used for pick and place applications.

During the last fifteen years, numerous electropneumatic positioning systems have appeared on the market and, at the present time, most of pneumatic manufacturers have on offer one or several arrangements prepared for point-to-point control or position tracking. Nevertheless, industrial positioning applications have been served primarily by hydraulic and electric servo drives. The main reason for this is the difficulty in using compressed air as a control medium. Firstly, a pneumatic controlled drive has a very low stiffness, small natural damping, and a natural resonant frequency in the order of 10 Hz or less. And secondly, it is very difficult to predict accurately the inherent non-linear behavior of pneumatic systems in order to establish a control strategy.

However, the opportunity to produce low cost widely applicable pneumatic servo drives has attracted a considerable research interest. Pneumatic actuator steady-state performance can be determined in first approximation by coupling the actuator and the regulation valve. In this way a prediction of the real working conditions (i.e. input power, cycle time estimation, etc.) cannot be achieved, especially if the design specifications require fast operation of the system with common speed control layouts.

Although the linear models can only represent approximately the dynamics of the physical system, they have been used as an aid to the design of suitable control strategies for pneumatic servos (Weston et al, 1984; Virvalo, 1989 and Brun et al, 1999). Different non-linear control models have been proposed for describing the global behavior of the pneumatic chambers (Brun et al, 1999 and Scavarda et al, 1994), but often they are later linearized in the vicinity of an equilibrium position. Usually, these models produce an improved performance when used in position or tracking control, even considering the polytrophic hypothesis, the gas as perfect and some other simplifications.

The main loss of accuracy in predictive models of pneumatic systems is due to the lack of good models for gas thermodynamics, variable orifices and piston friction (Maré et al, 2000). The objective of this paper is to present a simple way of modeling these factors and their order of magnitude. The classical meter-out layout for speed control is used to show the method accuracy.

2 Gas Dynamics in Pneumatic Systems

In general, fluid system components of reduced characteristic length are supposed to be lumped parameter systems when the fluid conditions inside them

This manuscript was received on 29 January 2003 and was accepted after revision for publication on 23 October 2003

can be described as a function of time alone. Thus, an actuator chamber will be considered a concentrated pneumatic capacity, while a local flow resistance will be accepted to be a pneumatic resistance with the corresponding causality relationship. For some components of sufficient length (e.g. for transmission lines), a distributed parameter model has to be used. The characteristic equations for gases in pneumatic tubes can be found in literature (Arp, 1975).

The circuit that will be analyzed here is schematically shown in Fig. 1. It consists of a double acting pneumatic cylinder that is connected to a two-position five-way valve and a speed control valve. In modeling, it is accepted that the pneumatic chamber is a thermodynamic accumulator while passages through directional control valve act like pneumatic resistances.

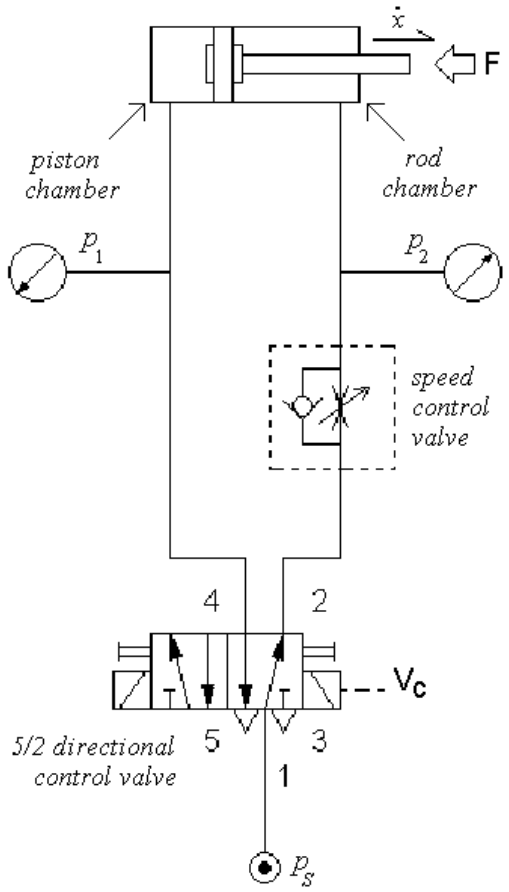

Fig. 1: *Pneumatic meter-out circuit for speed control*

A pneumatic chamber is a thermodynamic accumulator where the gas total energy, *E*, depends on the mass, *m*, contained in the volume, *V*, and the specific internal energy per unit mass, *e*. Inside the pneumatic chamber, the specific internal energy of the air, considered a homogeneous non-reactive substance, is defined by

$$e = u + \frac{v^2}{2} + g\,z \qquad (1)$$

The momentum variation will not be considered within the control volume and the global mass potential term, *z*, will be omitted in the following explanation. Changes in *E*, being then $E \approx U$, occur because of the convection of energy ($\dot{H}$), the heat conduction through the accumulator internal walls (Q_w) and the port (Q_c), and the boundary mechanical work ($p\dot{V}$). From a causality point of view, the mass and energy transport flows required for the pneumatic accumulator are outputs for the pneumatic resistance in conductance form. The sign of the mass flow, $\dot{m}$, is dictated by the sign of the pressure drop across the valve.

Basic models of pneumatic actuators chambers assume that the gas process in compression and expansion is polytrophic (Andersen, 1967 and Sorli et al, 1999). A common practice is to assume that the processes involved are isothermal, adiabatic or in general polytrophic. The polytrophic hypothesis guarantees good results in a fast and easy way by using mechanical variables (i.e., neither temperature nor enthalpy are needed), and not considering either the thermal and mechanical coupling or the gas thermal behavior. But the value of the polytrophic exponent used in calculations is often unknown and researchers have used different values that have proven in some cases to be inaccurate. For example, it has been found experimentally that the mean polytrophic exponent may exceed 1.8 when the non-ideal gas properties are considered in a real compression process (de las Heras, 1997).

The polytrophic exponent method has been progressively improved by considering, firstly, that the process is adiabatic with isentropic conditions and ideal gas (Wang et al, 1987). More recently, the isothermal model has been successfully used in designing position controllers (Scavarda et al, 1994). Ikeo (Ikeo et al, 1992) showed that the waveform of pressure and displacement agree well with experimental results when a polytrophic of $n = 1.1$ is selected. Unfortunately, such a partial description of chamber thermodynamics is not accurate enough to provide useful predictive models since Ikeo et al (1992) observed that it was not possible to predict the temperature waveforms using a polytrophic exponent. It is important to notice here that an expansion process with $n = 1.1$ in an open system, like the pneumatic chamber, could be closer to adiabatic than to isothermal.

Other models use the energy and conservation principles to develop the set of equations that relate pressure and temperature evolution during the overall process (Maré et al, 2000 and Kagawa et al, 1990). These models were not extended to the case of real gas and they do not use the thermal time constant for estimating the amount of heat transfer. The main virtue of the thermal time is that can be directly compared in magnitude with the process time in order to know if the process, in expansion or compression, could be considered adiabatic or not.

2.1 Temporal Changes of Thermodynamic Variables

The algorithm begins with the first principle applied to the pneumatic chamber. With the piston moving, the only mechanical work per time unit present is the $p\dot{V}$ term, and hence:

$$Q - p\dot{V} = \frac{d}{dt}\int_V \rho e\, dV + \int_\Omega \rho\left(e + \frac{p}{\rho}\right) v\, d\Omega \qquad (2)$$

The specific internal energy, *e*, appears in both integral terms in the right side of Eq. 2. The first right side term can be easily integrated if it is assumed that the product of density and specific energy is uniformly distributed inside the pneumatic chamber. This is acceptable for a discharge process when the ratio between the nozzle (or valve) area and the square of the chamber characteristic length is small and, consequently, local convective effects are only important in a small region near the outlet vent.

It is common to use the hypothesis of local equilibrium, which means that the process occurs as a succession of states in nearly static equilibrium. Although that is essentially incorrect, the continuous variation of the uniformly distributed average pressure can be admitted for small vessels. The same is not true for temperature because of the local differences of density caused by the flow and the heat transfer. However, following the explanations of Deckker and Chang (Deckker, 1968), it seems that the instantaneous temperature, as calculated from the experimental pressure, corresponds acceptably well to the average of the local temperatures experimentally measured. For the effect of the heat transfer near the wall the thermal boundary layer width, δ, can be estimated with Eq. 18 if one wants to take it into account when integrating Eq. 2.

In order to evaluate the convective term of Eq. 2, further considerations are required. The gas kinetic energy flow is much lower than the convected enthalpy flow in the inlet and outlet ports (about a thousand times). Nevertheless, the Reynolds number in control orifices is high enough in order to consider a uniform velocity distribution in the whole input and output sections. For that reason, with a uniform flow, the other thermodynamic variables are assumed to be uniform also in the cylinder ports and Eq. 2 can be completely integrated.

Furthermore, it is going to be assumed that the ambient conditions and supply pressure and temperature are constant (in experiments, a five-percent variation in pressure supply can be observed when movement begins due to system limited capacity effects). The possible internal and external leakage, the influence of pipe connections at the actuator inlets and the lumped resistive, inductive, capacitive or propagation effects in pipes are ignored. In practice the piston speed never exceeds a few meters per second and thus the gas kinetic energy is typically much lower than the intrinsic gas internal energy.

With the above assumptions: $e \approx u$. It is also assumed that properties of air flowing into the control volume, *V*, through the area, Ω, (subscript "i") are different from those inside, and those flowing out are the same as those inside. Then Eq. 2 becomes for a single input:

$$Q - p\dot{V} = \dot{U} - \dot{m}\left(u_i + \frac{p_i}{\rho_i}\right), \text{ with } m > 0 \qquad (3)$$

and for a single output:

$$Q - p\dot{V} = \dot{U} - \dot{m}\left(u + \frac{p}{\rho}\right), \text{ with } m < 0 \qquad (4)$$

The mass flow-rate has been taken positive when flowing into a pneumatic chamber. In this way, the instantaneous mass in each chamber can be calculated by:

$$m = m_0 + \int_0^t \dot{m}\, dt \qquad (5)$$

and the instantaneous volume is:

$$V = V_0 + \int_0^t \dot{V}\, dt \qquad (6)$$

The external heat, *Q*, in the previous relations takes into account the heat transfer between the air and the cylinder wall, and the heat conduction through the inlet and outlet ports:

$$Q = Q_w + Q_c \qquad (7)$$

The heat exchanged with the wall Q_w can be evaluated using the thermal constant time, τ_T, derived from the averaged heat-transfer coefficient of the cylinder surface by:

$$Q_w = \alpha A_w (T_w - T) = m c_v \frac{T_w - T}{\tau_T} \qquad (8)$$

Equation 3 and 4 can be rewritten using Eq. 7 to become:

$$\dot{U} = Q_w + \{\dot{m} h_i + Q_c\} - p\dot{V}, \text{ with } m > 0 \qquad (9)$$

$$\dot{U} = Q_w + \{\dot{m} h + Q_c\} - p\dot{V}, \text{ with } m < 0 \qquad (10)$$

The switching between Eq. 9 and 10 depends on the direction of flow, which is determined by a pressure balance between valve inlet and outlet. Here *h* is the gas enthalpy that can be calculated by $c_p T$, being c_p a function of temperature. This reticulation takes into account the total power transmitted through the valve ($\dot{m} h_i + Q_c$) and not just the enthalpy flow ($\dot{m} h$).

The conduction heat, Q_c, is assumed to be proportional to the temperature difference of the gas upstream and downstream the valve, i.e. inside and outside the chamber. It can be omitted in first approximation because it is only needed if one wants to simulate the total equilibrium in adiabatic conditions (if not, the gas cannot reach it). No real system is completely adiabatic, and that is the reason why there is always a thermodynamic flow (heat conduction, Q_w) leading the system to the total equilibrium condition where gas temperature equals wall temperature.

In practice it is better to work with temperatures and pressures instead of enthalpy. With:

$$\dot{U} = \dot{m} u + m \dot{u} \qquad (11)$$

and, for a real gas (all properties referred to the gas inside the pneumatic chamber):

$$du = c_v\, dT + \left[T \left.\frac{\partial p}{\partial T}\right|_{\rho} - p \right] d\left(\frac{1}{\rho}\right) \tag{12}$$

it is easy to transform Eq. 9 and 10 into the form (without heat conduction, Q_c):

$$\dot{T} = \frac{1}{m c_v}\left\{ \alpha A_w (T_w - T) + (h_S - h)\dot{m} + T \left.\frac{\partial p}{\partial T}\right|_{\rho} \left(\frac{\dot{m}}{\rho} - \dot{V} \right) \right\} \tag{13}$$

with $m > 0$, and

$$\dot{T} = \frac{1}{m c_v}\left\{ \alpha A_w (T_w - T) + T \left.\frac{\partial p}{\partial T}\right|_{\rho} \left(\frac{\dot{m}}{\rho} - \dot{V} \right) \right\} \tag{14}$$

with $m < 0$.

The pressure is derived integrating $\dot{T}$ and using the desired gas state law and the corresponding initial condition and gas density. The mean gas density is being calculated at every integration step with Eq. 5 and the instantaneous volume from Eq. 6, depending on piston speed and the corresponding piston area.

Since for an ideal gas,

$$T \left.\frac{\partial p}{\partial T}\right|_{\rho} = p \tag{15}$$

the Eq. 13 and 14 become, using again Eq. 8

$$\dot{T} = \frac{T_w - T}{\tau_T} - \frac{1}{m c_v}\left\{ p\left(\dot{V} - \frac{\dot{m}}{\rho} \right) - c_p (T_S - T)\dot{m} \right\} \tag{16}$$

with $m > 0$, and

$$\dot{T} = \frac{T_w - T}{\tau_T} - \frac{1}{m c_v}\left\{ p\left(\dot{V} - \frac{\dot{m}}{\rho} \right) \right\} \tag{17}$$

with $m < 0$.

This reticulation replaces the usual polytrophic relation between gas volume and pressure. Furthermore, it allows working with temperatures (even in the real gas case with Eq. 13 and 14), and uses the thermal constant time for estimating the heat exchanged with the surroundings. The amount of heat transfer depends on the mechanical process time or frequency, but an exact value of the thermal time constant is not needed when modeling if one compares its order of magnitude with other characteristics times. For example, an isothermal process occurs when the thermal time constant, τ_T, is an order of magnitude lower than the characteristic mechanical process time, usually the process time: τ. Pourmovahed and Otis first introduced the thermal constant time for pneumatic accumulators (Pourmovahed et al, 1990).

In transient thermal processes it is often assumed that the process is isothermal near the wall and tends to be isentropic further towards the internal region of the volume. The thermal boundary layer width, δ, is being estimated by

$$\delta \approx \frac{L}{(\mathrm{Re}\ \mathrm{Pr})^{1/2}} = \left(\frac{k_0 \tau}{\rho_0 c_{p0}} \right)^{1/2} \tag{18}$$

In the case of pneumatic systems, τ is the process time and it usually depends on valve size, thermodynamic stagnation conditions and cylinder geometry. The order of magnitude of τ is estimated by

$$\mathrm{O}(\tau) = \frac{V}{\gamma C\, p_N} \tag{19}$$

Thus, δ can be calculated with variables in the steady state stagnation condition. For example, with air at normal conditions (Pr = 0.69), a volume of characteristic length 0.1 meters and time τ equal to 0.25 seconds (Re = 2600), the wall thermal effect penetrates the vessel 2.4 millimeters. With air at 7 bar abs, δ becomes only 1 millimeter and the process would be nearly isentropic inside of the cylinder. In conventional industrial applications where process times are getting smaller as systems become faster, the adiabatic approximation works well because there is not enough time to transfer heat ($\tau_T > \tau$). Thus, why does an isothermal polytrophic index of 1.1 fit experimental data?

2.2 About the Instantaneous Polytrophic Index

It is accepted that the polytrophic index indicates the amount of heat received by the gas and it has been used in both open and closed pneumatic systems. The polytrophic relationship can be written

$$\frac{p_1}{{\rho_1}^n} = \frac{p_2}{{\rho_2}^n} \tag{20}$$

Equation 21 could also be used in order to describe a polytrophic process if one considers that $p = \rho RT$ is valid between two states (1, 2) separated by time Δt.

$$\frac{T_1}{{\rho_1}^{n-1}} = \frac{T_2}{{\rho_2}^{n-1}} \tag{21}$$

Deriving Eq. 20 and 21, assuming n to be constant in Δt, we obtain:

$$n = \frac{\dot{p}/p}{\dot{\rho}/\rho} = 1 + \frac{\dot{T}/T}{\dot{\rho}/\rho} \tag{22}$$

which is easy to introduce into a computer program (see Eq. 13 or Eq. 16).

This equation is worth considering with a little thoroughness. The state equation for an ideal gas and the Gibbs equation for the internal energy, both expressed per unit of mass and time and using the specific volume, $\upsilon = 1/\rho$, are:

$$\dot{p}\upsilon + p\dot{\upsilon} = R\dot{T} \tag{23}$$

$$T\,\dot{s} - p\dot{\upsilon} = \dot{u} = c_v\,\dot{T} \tag{24}$$

Equation 23 and 24 combined give

$$\dot{p}\upsilon + p\dot{\upsilon} = \frac{R}{c_v}\left(T\,\dot{s} - p\dot{\upsilon} \right) \tag{25}$$

Dividing by $p\dot{\upsilon}$ and including Eq. 22, we get:

$$n = \gamma - \frac{R}{c_v}\frac{T\,\dot{s}}{p\dot{\upsilon}} \tag{26}$$

An equation equivalent to Eq. 26 for real gases as a function of the compressibility factor, *z*, defined in $p = z\,\rho\,R\,T$, has been derived by de las Heras (de las Heras, 1997). In the same reference, the $T\,\dot{s}$ product for an amount of mass of gas *m* contained in a variable volume chamber in a quasi-static charging process is deduced to be

$$T\,\dot{s} = \frac{1}{m}\left(\dot{m}(h_S - h) + \dot{Q}_w\right) \tag{27}$$

The $T\,\dot{s}$ product is calculated while discharging by

$$T\,\dot{s} = \frac{1}{m}\dot{Q}_w \tag{28}$$

Therefore, using Eq. 27 and 28, it is possible to adapt Eq. 26 for both processes. Then

$$n = \gamma - \frac{R}{c_v}\left(\frac{\dot{m}(h_S - h) + \dot{Q}_w}{p\left(\dot{V} - \frac{\dot{m}}{\rho}\right)}\right) \tag{29}$$

is valid for the air in the pneumatic chamber when the flow comes in, and

$$n = \gamma - \frac{R}{c_v}\left(\frac{\dot{Q}_w}{p\left(\dot{V} - \frac{\dot{m}}{\rho}\right)}\right) \tag{30}$$

has to be used when the air is emptying the chamber.

It is evident now from Eq. 29 that an adiabatic loading process (with $\dot{Q}_w \equiv 0$) is not with $n \equiv \gamma$ because of the existence of enthalpy flow. In an adiabatic and reversible discharging process the specific entropy remains constant following Eq. 28 and $n \equiv \gamma$ from Eq. 30, but not the total entropy since the system is losing mass.

An analysis of the mean order of magnitude of the terms in Eq. 29, for $\tau_T \approx 1.1\,\tau$, shows that

$$\frac{\mathrm{O}\left(\dot{m}(h_S - h) + Q_w\right)}{\mathrm{O}\left(p\left(\dot{V} - \frac{\dot{m}}{\rho}\right)\right)} = \frac{\frac{\gamma}{\gamma - 1} C\,p_N\,p_S\left(1 - \frac{\tau}{\tau_T}\right)}{(\gamma - 1) C\,p_N\,p_S} \approx \frac{3}{4} \tag{31}$$

Ikeo et al (1992) results are confirmed with

$$\mathrm{O}(n) \approx \gamma - \frac{R}{c_v}\left(\frac{3}{4}\right) \approx 1.1 \tag{32}$$

As demonstrated, (de las Heras, 1997), when the internal irreversibilities are included in Eq. 27 and 28, the polytrophic index can be bigger than the specific heat ratio, which until now was accepted to be the polytrophic upper limit for the ideal gas.

2.3 Compressible Flow through Valves and Orifices

The International Standard ISO 6358 (1989) introduces a simple analytic method for controlling, measuring, conducting or guiding the air flow in pneumatic circuits which is directly applicable to all types of pneumatic components. This pattern establishes a simplification of the theoretical equation for the isentropic mass flow rate of compressible fluid through convergent nozzles first obtained by Saint-Venant in 1839. When the upstream Mach number can not be neglected, the mass flow rate was deduced by Mo (Mo, 1989).

The non-ideal nature of real gases and the fact that the expansion process cannot be regarded as isentropic deflect the real behaviour of the nozzle from the theoretic characteristic obtained by Saint-Venant. The real flow path is adapted by using two experimental coefficients: the sonic conductance *C* and the critical pressure ratio *b*. The ISO 6358 shows how to obtain these parameters by means of tests at steady flow.

Recently, an alternative method for obtaining the sonic conductance of pneumatic valves, *C*, has been presented (de las Heras, 2001). This new method uses the characteristic unloading time defined in a transitory discharge process and proposes an experimental procedure at lower cost than the ISO 6358. Furthermore, with this method the test rig needed is not so large and a precise measure of the variables involved in the discharge, pressure, mean temperature or specific volume, is not required either.

The maximum theoretical mass flow rate is obtained for chocked flow, with $r \equiv b = \frac{p_{2s}}{p_1} = 0.52$, for γ = 1.4. When a gas expands in a convergent nozzle it is not possible to take a pressure at outlet p_2 lower than the value p_{2s}, which corresponds to the maximum mass flow rate, because the pressure wave for the decrease of p_2 does not come back upstream. In other words, the flowing gas does not perceive that the downstream pressure has decreased because is moving at the speed of sound. In the subsonic path, where $r = \frac{p_2}{p_1} > b$, the flow-mass rate drops nearly elliptically with *r* increasing, and so it is reasonable to define the term

$$\omega = \sqrt{1 - \left(\frac{r - b}{1 - b}\right)^2} \tag{33}$$

Generally, the method presents the following formulation in terms of the valve conductance, *C*. The mass flow rate is:

$$\dot{m} = C\,K_T\,\rho_N\,p_1\,\omega \tag{34}$$

where ω is obtained from Eq. 33 in the subsonic case, and the stagnation temperature correcting ratio is:

$$K_T = \sqrt{\frac{T_N}{T_1}} \tag{35}$$

when $r < b$ the flow is choked and $\omega = 1$.

It is usually accepted that the nozzle geometry is a very important local factor in the mass flow rate characteristic. Definition of *C* in the ISO Standard is based on test conditions at steady flow in which the upstream pressure is maintained constant, and consequently, the nozzle perceives a system with infinite capacity.

The contributions of the adjacent chamber of vol-

ume V and capacitance C, and the resistance associated with the system valve-line, R, are included in the determination of C when the study is carried out by means of the unloading characteristic time, τ_U. It has been demonstrated recently (de las Heras, 2001), that the equivalent sonic conductance of the RC pneumatic system can be evaluated using the expression:

$$C = \frac{K_{T0} V}{\gamma p_N} \frac{1}{\tau_U} \propto \frac{1}{\tau_U} \qquad (36)$$

This is a direct consequence of the C dependence on the RC system time, τ_U. In this way, any given pneumatic element will conduct different flow rates depending on the system to which it is connected to and, consequently, it is not possible to determine the true effective conductance of the element by the steady flow test indicated by ISO 6358. Furthermore, the sonic conductance obtained by Eq. 36 is smaller than the one obtained by the ISO 6358, and explains why the effective mass flow through some valves is significantly smaller than one expected when using the C estimation suggested by the ISO Standard.

3 Model Experimental Validation

Test circuit is shown in Fig. 1. A speed control valve in meter-out layout controls the cylinder speed. This is the way used in most common industrial applications because it is accepted that the actuator speed gets bigger increasing supply pressure. With meter-out regulation, both chamber pressures are high enough to reduce the influence of friction variation due to changes in ambient, seal and wall temperatures. Furthermore, cylinder speed can be controlled and stick-slip phenomenon is avoided except for extremely low velocities.

The conductance of the speed control valve in Fig. 1 was found to be a function of the valve switch positions (Table 1). The critical pressure ratio resulted of 0.3 for both flow valves. The main data concerning the actuator and working conditions have been summarized in Table 2.

The sliding friction model is reduced to Eq. 37 wherein the sliding coefficients have been evaluated by adjusting the experimental data (Fig. 2). Karnopp's approach (Karnopp, 1985) was used for the stick friction model due to its proved computational efficiency (Haessing et al, 1991). The results of tests show that Coulomb friction level at zero velocity is influenced by the mean value of chamber pressures (p_1+p_2) due to sealing design and its effect on normal force distribution. On the other hand, the pressure difference (p_1–p_2) approximates the slope of the viscous friction. In fact, both pressures do not have the same effect in sliding, probably due to seal asymmetries and to a non-uniform lubrication (coefficient k_4 in Eq. 37). The effective elasticity modulus of the materials in contact was verified by Virto to be the most significant magnitude of the sliding (Virto et al, 2000).

$$F_f = \{k_0 + k_1(p_1 + p_2)\} + \{k_2 + k_3(p_1 - k_4 p_2)\} v \qquad (37)$$

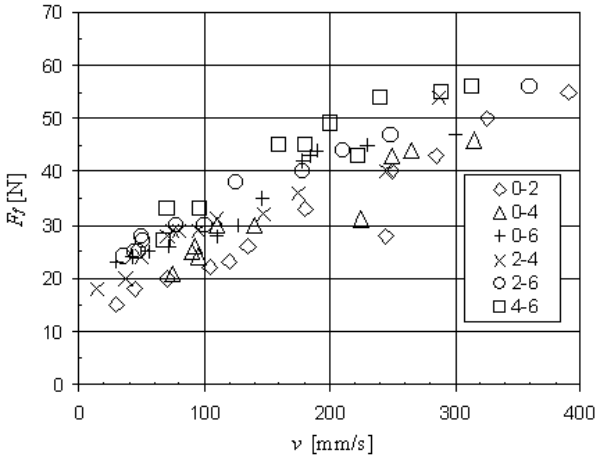

Fig. 2: *Friction force data for the actuator (label is p_1-p_2 bar, positive direction of sliding)*

Experiments were carried out for all the positions (from switch 1 to 4) of the speed control valve and for 4 and 7 bar absolute supply pressures. In initial condition, the command V_C to the 5/2 valve is absent and the piston is retracted. The signal V_C causes the rod extends and the start of data acquisition. After that, chamber pressures and the actuator stroke and velocity were recorded during some cycles of operation and the cycle mean times computed and compared with the simulated ones. In Fig. 3 measured velocity is compared with the simulated one. It can be observed that both curves agree quite well over the cycle.

Table 1: Speed control valve conductance for four valve positions

Valve positions	C [L/min/bar]
Switch 4	1.41
Switch 3	2.68
Switch 2	13.2
Switch 1	210

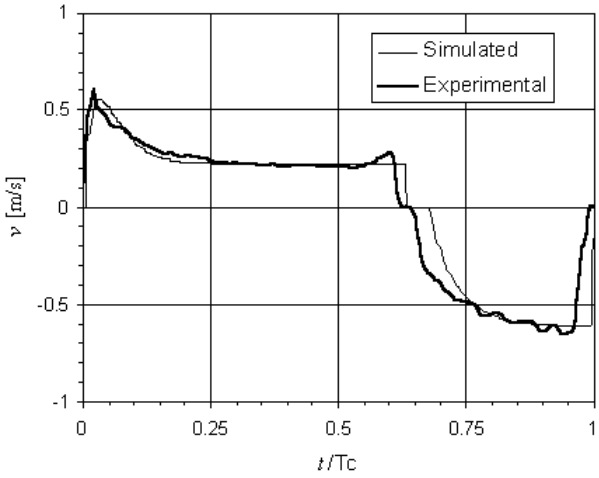

Fig. 3: *Actual and simulated velocity during a cycle for switch 2 and p_S=4 bar abs (Tc (exp) = 2.62 s)*

Table 2: System data during experimental tests and used in simulation

Actuator total stroke	450	mm
Piston diameter	45	mm
Rod diameter	15	mm
External force	0	N
Atmospheric pressure	0.98	bar
Ambient temperature	292	K
Thermal constant time	5	s
Directional control valve conductance (all bias)	490	L/min/bar
Speed control valve conductance	See Table 1	

Cycle times obtained from experiments are compared with the simulation results in Fig. 4 and 5. Deviations between the actual and simulated cycle times are less than 3.5 % for all the cases. However, it is interesting to note that the cycle time was quite similar for both supply pressure with all the positions of the speed control valve. For example, one can observe in Fig. 5 that when supply pressure changes from 4 to 7 bar, the result is only a ten-percent cycle time decrease. We can also observe that the plot of cycle time vs. valve conductance follows a hyperbolic law: a decrease in cycle time needs an increase in valve conductance, and hardware fixes the limits.

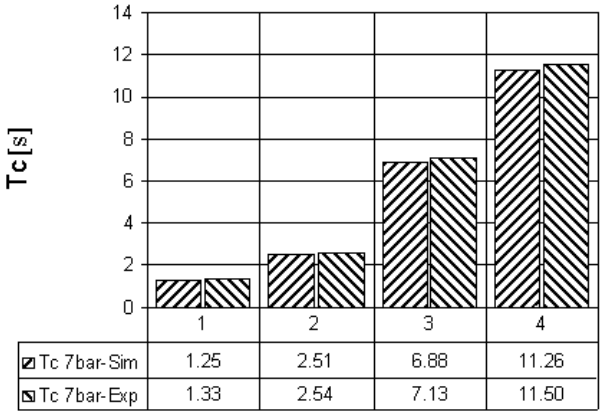

Fig. 4: *Cycle times vs speed control valve switch for experimental and simulated results (p_S = 7 bar abs)*

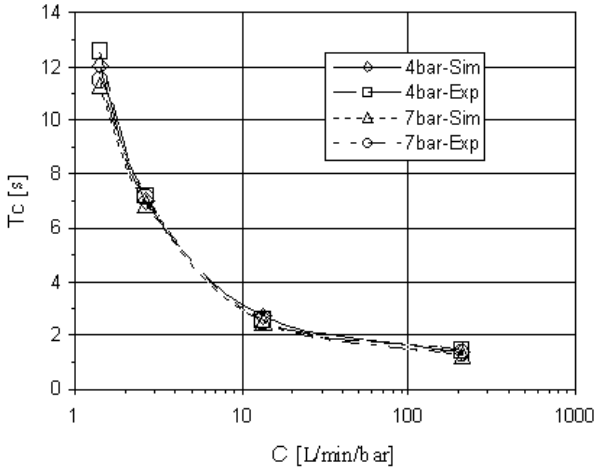

Fig. 5: *Cycle times for experimental and simulated results vs. control valve conductance for 4 and 7 bar*

In Fig. 6 the trajectory lines obtained for the four positions of the speed control valve are showed. A good agreement can be observed concerning the shapes of the response. A steady-state motion follows the quick start-up, where the velocity is function of conductance of the control valve and the rod chamber pressure. It is been observed that during the start-up in meter-out circuits the pressure in the piston chamber increases quickly. Cushion effect generated by the movement of the piston compressing air in the rod chamber is more evident for small speed control valve conductances (valve positions 3 and 4).

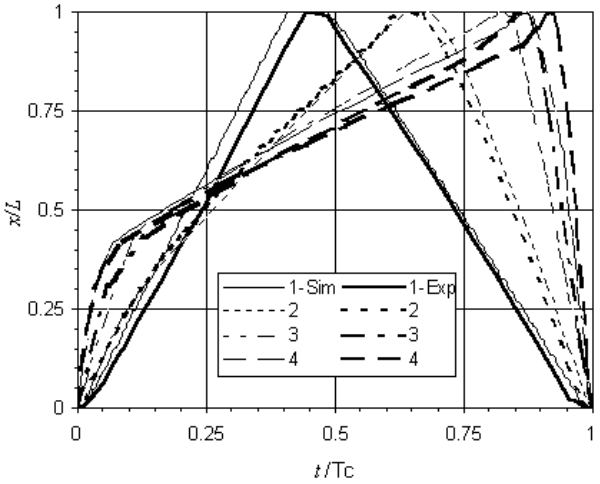

Fig. 6: *Normalized trajectory lines for the four switch positions of the speed control valve and p_S = 4 bar abs*

Although it is not evident from Fig. 6, the initial piston movement is identical for all the positions of the speed control valve until pressure in the rod chamber reaches the stationary value. This shows the inadequacy of meter-out velocity regulation for short actuators where the steady-state movement will not be achieved. The cushion effect is not present in meter-in regulation where the steady-state is achieved quickly and, for this reason, the cycle time is not much longer in meter-in than in meter-out circuits, and the control over the piston velocity becomes easier.

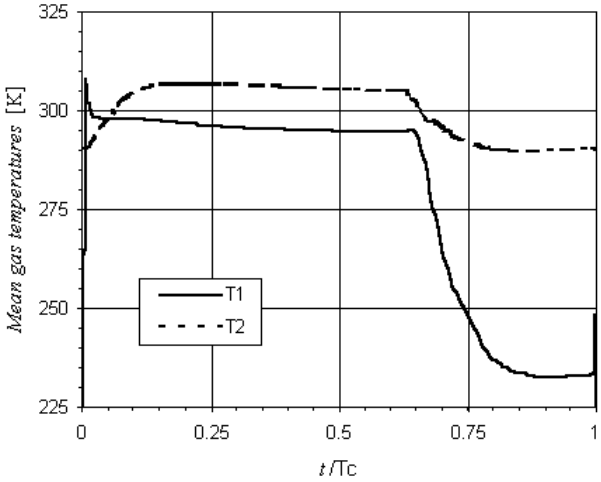

Fig. 7: *Simulated mean gas temperatures during a cycle for switch 2 and p_S = 4 bar abs*

Figure 7 and 8 show the predicted results obtained for the averaged gas temperature and polytrophic index for each chamber. After the quick start-up in both directions of movement, the simulated mean gas temperature appears to reach a stationary value. Looking at the instantaneous polytrophic index changes shown in Fig. 8, it is evident that the polytrophic index is not constant. However, a mean polytrophic index of 1.1 fits experimental data, as it has already been said, and can be used for designing proposes. The low-level temperature value obtained for the piston chamber when the rod starts the return movement it is also significant because it falls down to 235 K. This is a consequence of the quick discharge of air contained in this chamber. Pressure p_1 drops from supply pressure to exhaust pressure, and can produce condensation of water. Air in the rod chamber does not become so cool because pressure p_2 held at almost the same value for full cycle in meter-out layouts.

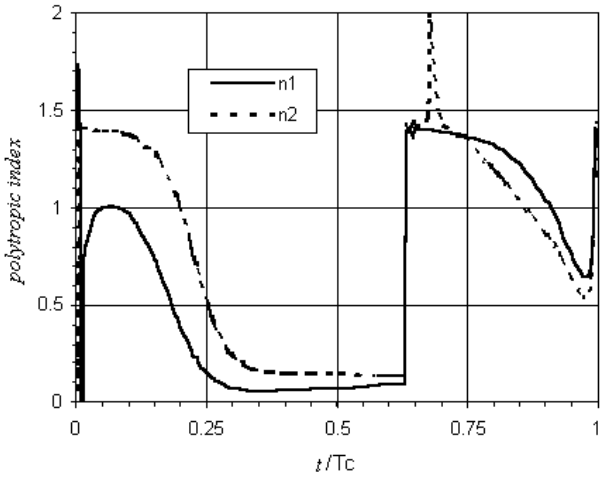

Fig. 8: *Simulated instantaneous polytrophic index during a cycle for switch 2 and p_S = 4 bar abs*

When the piston movement begins, the polytrophic index n_1 tends to reach the isothermal value as air contained in the piston chamber is pressurized as it is observed in Fig. 8. Meanwhile, in the rod chamber the polytrophic n_2 increases to 1.4 and remains at this value until steady-state motion of piston is achieved and pressure p_2 remains practically constant. The polytrophic index can be estimated using Eq. 29 and 30 if the system can be considered adiabatic, i.e., while $t << \tau_T$.

During the return stroke the piston chamber is depressurised quickly. For the rod chamber, one can expect n_2 reaching the isothermal level (because is charging and n_1 reached it in the forward movement) but the simulated value is about 1.4. This is a consequence of the comparison in magnitude of numerator and denominator of Eq. 29. The quick return motion observed in meter-out circuits is caused mainly by the fast relaxation of air in the piston chamber while is being depressurised. Being the rod chamber pressure similar to the supply pressure when the return stroke begins (i.e., $p_2 \approx p_S$), the flow incoming the rod chamber is $m \approx 0$. Using Eq. 29, we deduce that $p\dot{V} >> \dot{m}(h_S - h) + \dot{Q}_w \approx 0$ and then $n_2 \approx \gamma$. Obviously, when $\dot{V} - \frac{\dot{m}}{\rho} \equiv 0$, i.e., the gas density is constant, the polytrophic n_2 of the rod chamber grows up to infinite. During the return stroke the polytrophic index of the piston chamber follows Eq. 30 in an adiabatic process and, hence, $n_1 \approx \gamma$.

4 Conclusions

The air compression process and fluid flow in pneumatic systems has been discussed in this paper. Useful relationships that will help designers to improve their models using real gas state laws, gas interrelation with its surroundings by the thermal time constant, and the total energy transmitted at the ports have been presented. Pneumatic models should incorporate a stick-slip friction algorithm in order to adjust the actuator complete dynamics.

The method presented in this paper allows the accurate prediction of cycle times. The accuracy of the algorithm was confirmed by experiments and can be a good reference point for understanding the pneumatic servomechanisms in which the compressibility effects are important, and the volume of the fluid concerned is variable. Models developed using this paper could be structured as a component library and used to identify the behaviour of more complex systems.

Nomenclature

b	critical pressure ratio	[-]
v	gas velocity	[m/s]
c_v	gas specific heat at constant volume	[J/kg/K]
c_p	gas specific heat at constant pressure	[J/kg/K]
e	specific internal energy	[J/kg]
g	gravity	[m/s^2]
h	specific enthalpy	[J/kg/K]
k	gas conductivity	[J/m/K/s]
m	mass of gas	[kg]
n	mean instantaneous polytrophic index	[-]
p	mean absolute gas pressure	[Pa]
r	pressure ratio	[-]
s	gas specific entropy	[J/kg/K]
t	time	[s]
u	specific intrinsecal internal energy	[J/kg/K]
z	compressibility factor	[-]
A	equivalent valve area, nozzle area	[m^2]
C	sonic conductance	[m^3/s/Pa]
E	gas total internal energy	[J]
F	force	[N]
K	gas characteristic constant	[sK$^{1/2}$/m]
L	characteristic length	[m]
$O(\ )$	order of magnitude operator	
Pr	Prandtl number, Pr = $c_p\mu/k$	[-]
Q	amount of heat exchanged per unit of time	[J/s]
R	gas constant	[J/kg/K]

Re	Reynolds number, $Re = \rho L^2/\mu\tau$	[-]
T	spatially averaged absolute gas temperature	[K]
Tc	cycle time	[s]
$\dot{H}$	enthalpic flow	[J/s]
$\dot{m}$	mass flow rate	[kg/s]
$\dot{V}$	volume change rate	[m^3/s]
α	averaged heat-transfer coefficient	[$J/m^2/K/s$]
δ	thermal boundary layer width	[m]
γ	gas specific heat ratio	[-]
μ	gas dynamic viscosity	[kg/m/s]
ω	subsonic term defined in Eq. 33	[-]
ρ	spatially averaged gas density	[kg/m^3]
τ	characteristic time	[s]
Ω	generic surface	[m^2]

Subscripts

0	stagnation condition, initial condition
1	up-stream, actuator piston chamber
2	down-stream, actuator rod chamber
atm	atmosphere
exp	experimental
f	friction
i	air flowing into the chamber
s	sonic condition, sound
w	wall
E	exhaust port
N	normal condition
S	supply port
T	temperature, thermal
U	Unloading/discharging

References

Andersen, B. 1967. *The analysis and Design of Pneumatic Systems*. John Wiley and Sons. NY.

Arp, V. 1975. Thermodynamics of Single-Phase One-Dimensional Fluid Flow. *Cryogenics*, May, pp 285-289.

Brun, X., Belgharbi, M., Sesmat, S., Thomasset. D. and **Scavarda, S.** 1999. Control of an Electropneumatic Actuator: Comparison Between Some Linear and Non-linear Control Laws. *Proc. ImechE*, Part I, Vol. 213, pp. 387-406.

de las Heras, S. 1997. *Optimización de Suspensiones Hidroneumáticas con Amortiguador Integrado*. Ph.D. thesis, UPC, Terrassa.

de las Heras, S. 2001. A New Experimental Algorithm for the Evaluation of the True Sonic Conductance of Pneumatic Components Using the Characteristic Unloading Time. *International Journal of Fluid Power*, Vol. 2, No.1, pp. 17-24.

Deckker, Chang 1968. Transient Effects in the Discharge of Compressed Air From a Cylinder Through an Orifice. *Transactions of the ASME, Journal of Basic Engineering*, pp. 333-342.

Haessig, D. A. Jr. and **Friedland, B.** 1991. On the Modeling and Simulation of Friction. *Transactions of the ASME, Journal of Dynamic Systems*, Measurement and Control, Vol. 113, pp. 354-362.

Ikeo, S., Zhang, H., Takahashi, K. and **Sakurai, Y.** 1992. Simulation of Pneumatic Systems using BGSP (Bond Graph Simulation Program). *5th Bath International Workshop in Circuit, Components and System Design*.

International Standard ISO 6358. 1989. Pneumatic Fluid Power-Components Using Compressible Fluids. Determination of Flow-Rate Characteristics.

Kagawa, T. and **Ohligschläger, O.** 1990. Simulationsmodell für Pneumatische Zylinderantriebe. *Ölhydraulik und Pneumatik*, Vol. 34. pp. 115-120.

Karnopp, D. 1985. Computer Simulation of Stick-Slip Friction in Mechanical Dynamic Systems. *Transactions of the ASME, Journal of Dynamic Systems, Measurement and Control*, Vol. 107, pp. 100-103.

Maré, J-C., Geider, O. and **Colin, S.** 2000. An Improved Dynamic Model of Pneumatic Actuators. *International Journal of Fluid Power*, Vol. 1, No. 2, pp 39-47.

Mo, J. 1989. Analysis of Compressed Air Flow Through a Spool Valve. *Proc. IMechE*, Part C, Vol. 203, pp. 121-131.

Pourmovahed, A. and **Otis, D. R.** 1990. An Experimental Thermal Time-Constant Correlation for Hydraulic Accumulators. *Transactions of the ASME, Journal of Dynamic Systems, Measurement and Control*, Vol. 112, pp. 116-121.

Scavarda, S. and **Richard, E.** 1994. Non linear Control of Electropneumatic and Electrohydraulic Servodrives: A Comparison. *11th Aachener Fluidtechnisches Koloquium*, Aachen, pp. 223-236.

Sorli, M., Gastaldi, L., Codina, E. and **de las Heras, S.** 1999. Dynamic Analysis of Pneumatic Actuators. *Simulation Practice and Theory*, Special Issue on Bondgraphs for Modeling and Simulation, Vol. 7, pp. 589-602.

Virvalo, T. 1989. Designing a pneumatic position servo system. *Power International*, June, pp. 141-147.

Virto, L. and **Arun, N.** 2000. Frictional Behaviour of Textile Fabrics. Part II: Dynamic Response for Sliding Friction. *Textil Research Journal*, Vol. 70, pp. 256-260.

Wang, Y. and **Singh, R.** 1987. Frequency Response of a Nonlinear Pneumatic System. *Transactions of the ASME, Journal of Applied Mechanics*, Vol. 54, pp. 209-214.

Weston, B., Moore, P., Thatcher, T. and **Morgan, G.** 1984. Computer Controlled Pneumatic Servo Drives. *Proc. IMechE*, Part B, Vol. 198, pp. 275-281.

Salvador de las Heras
Born May 18, 1967 in Vitoria (Spain). Mechanical engineer diploma in 1991, he got his Doctorate of Science in 1996 dealing with modeling, simulation and design optimization by bondgraphs of a hydro-pneumatic suspension for heavy vehicles. Professor in Fluid Mechanics and Hydraulic Systems at the Polytechnic University of Catalonia (UPC), his research activity is focused on advanced control of hydraulics and pneumatics systems.